University Technology Malaysia

From the SelectedWorks of Hadi Nur

May, 2006

Sulphated AlMCM-41: Mesoporous solid Brønsted acid catalyst for dibenzoylation of biphenyl

Eng Ng Poh, *Universiti Teknologi Malaysia*
Hadi Nur, *Universiti Teknologi Malaysia*
Mohd Nazlan Mohd Muhid, *Universiti Teknologi Malaysia*
Halimaton Hamdan, *Universiti Teknologi Malaysia*

Available at: https://works.bepress.com/hadi_nur/4/

Available online at www.sciencedirect.com
SCIENCE DIRECT
Catalysis Today 114 (2006) 257–262
CATALYSIS TODAY
www.elsevier.com/locate/cattod

Sulphated AlMCM-41: Mesoporous solid Brønsted acid catalyst for dibenzoylation of biphenyl

Ng Eng Poh, Hadi Nur, Mohd Nazlan Mohd Muhid, Halimaton Hamdan *

Ibnu Sina Institute for Fundamental Science Studies, Universiti Teknologi Malaysia, 81310 UTM Skudai, Johor, Malaysia

Abstract

Sulphated mesoporous solid Brønsted acid catalyst (SO_4-AlMCM-41) was prepared by impregnation of sulphuric acid on the surface of H-AlMCM-41. Characterization of SO_4-AlMCM-41 by pyridine adsorption studies and ^{27}Al MAS NMR showed that the presence of Brønsted acidity was correlated with octahedrally coordinated aluminium and solvent environment. Catalytic study demonstrated that the SO_4-AlMCM-41 catalyst has a higher activity in the dibenzoylation of biphenyl with benzoyl chloride than sulphuric acid, H-AlMCM-41 and sulphated amorphous silica.
© 2006 Elsevier B.V. All rights reserved.

Keywords: Sulphated AlMCM-41; Brønsted acidity; Dibenzoylation; Biphenyl

1. Introduction

Benzoylation is an important Friedel-Crafts acylation used in the commercial production of important chemicals such as benzophenone and its substituted analogues as additives in the synthesis of fine chemicals and dyes [1–5]. Recent interest is on the dibenzoylation of biphenyl with benzoyl chloride, from which the monosubstituted product, 4-phenyl-benzophenone or 4-benzoylbiphenyl (4-PBP), a useful precursor in perfumes, and the disubstituted product, 4,4′-dibenzoylbiphenyl (4,4′-DBBP), an important monomer in the polymerisation of poly(4,4′-diphenylene diphenylvinylene) or namely PDPV are formed [6–8].

Current production of disubstituted 4,4′-DBBP is still via the difficult homogeneously catalysed process [6]. Despite the increase of research activities in the field of heterogeneous catalysis, synthesis of disubstituted compound using zeolite has not so far been successful. Although heterogeneously catalysed reactions using microporous molecular sieve did not show much potential, the large internal surface area and channel apertures of mesoporous molecular sieve MCM-41 is a promising alternative for reactions involving large molecules. Purely siliceous MCM-41 materials have no substantial acidity, and so there is continuing interest in the incorporation of metal or non-metal in order to create acid sites. Besides, the presence of Brønsted and Lewis acid sites in H-AlMCM-41 play significant roles in enhancement of the catalytic activity and adsorptive capacity [9–11].

The first example of successful formation of disubstituted 4,4′-DBBP catalysed by mesoporous H-AlMCM-41 with 100% selectivity was reported; however, with very low conversion (0.05%) [9–10]. Recently, a number of studies on sulphation of AlMCM-41, in order to increase the acidity, have been reported [12–16]. However, they demonstrated that the sulphated AlMCM-41 only exhibits Lewis acidity.

In this work, we present a simple preparation method to generate solid Brønsted acid catalyst by introducing sulphate groups onto the surface of AlMCM-41. The catalytic activity of the sulphated AlMCM-41 was studied in the dibenzoylation of biphenyl with benzoyl chloride reaction. The results obtained over sulphated AlMCM-41 were compared with those obtained using sulphuric acid, H-AlMCM-41 and sulphated amorphous silica.

2. Experimental

2.1. Synthesis of AlMCM-41

The AlMCM-41 with SiO_2/Al_2O_3 of 15 was synthesized according to established procedure [9]. Sodium silicate was prepared by dissolving 6.13 g of rice husk ash (97% SiO_2) and

* Corresponding author. Tel.: +607 5536060; fax: +607 5536080.
E-mail address: hali@kimia.fs.utm.my (H. Hamdan).

0920-5861/$ – see front matter © 2006 Elsevier B.V. All rights reserved.
doi:10.1016/j.cattod.2006.01.010

2.00 g of NaOH in 40 ml distilled water at 80 °C for 2 h under stirring. The resulting solution was labelled as solution A. Another solution (solution B) was prepared by mixing 0.7558 g of $NaAlO_2$ (Riedel-de-Haän®, 50–56% Al_2O_3), 6.07 g of CTABr and 0.70 g of NH_4OH 25 wt.% in 35 ml distilled water, followed by stirring at 80 °C until a clear solution was obtained. Both solutions A and B were mixed together in a polypropylene bottle to give a gel with a composition of 6 SiO_2:CTABr:1.5 Na_2O:0.15 $(NH_4)_2O$:250 H_2O, followed by vigorous stirring. The resulting gel was kept in an air oven for crystallization at 100 °C for 24 h. The gel was then cooled to room temperature and the pH of the gel was adjusted close to 10.2 by adding 25 wt.% acetic acid. The heating and pH adjustment was repeated twice. The solid product was filtered, washed, neutralized and dried overnight at 100 °C. Finally, the solid product was calcined at 550 °C in air for 10 h in order to remove the trapped organic template. The products before and after calcination are labelled as *uncal*-AlMCM-41 and *cal*-AlMCM-41, respectively.

2.2. Preparation of H-AlMCM-41 and sulphated AlMCM-41

H-AlMCM-41 mesoporous material was prepared by ion-exchange of 0.70 g *cal*-AlMCM-41 sample with 50 ml of 0.2 M NH_4NO_3 at 60 °C for 6 h. The solid was filtered, washed with deionized water and dried at 110 °C for 2 h. The ion-exchange was repeated three times. H-AlMCM-41 was then calcined at 550 °C. Sulphation of H-AlMCM-41 was carried out by adding H-AlMCM-41 (0.50 g) to 10 ml toluene and 30 μl H_2SO_4 (95–97%) in a round bottom flask. The mixture was stirred at 50 °C for 1.5 h and dried at 130 °C for 12 h. The sulphated AlMCM-41 is labelled as SO_4-AlMCM-41.

2.3. Characterization of the mesoporous materials

MCM-41 mesoporous materials were characterized by powdered X-ray Diffraction (XRD) using a Bruker Advance D8 using Siemens 5000 diffractometer with Cu K_α radiation (λ = 1.5418 Å, 40 kV, 40 mA). Infrared spectra were acquired by using a Perkin Elmer Spectrum One FT-IR spectrometer with a 4 cm^{-1} resolution and 10 scans in the mid IR region (400–4000 cm^{-1}). ^{27}Al MAS NMR spectra were recorded using a Bruker Ultrashield 400 spectrometer at a frequency of 104.2 MHz with a spin rate of 7 kHz, pulse length of 1.9 μs, relaxation time delay of 2 s and 6000 scans. The chemical shifts of ^{27}Al were reported in relation to $Al(H_2O)^{3+}$. TG-DTA measurements were carried out on a Perkin Elmer's Pyris Diamond Thermogravimetric/Differential Thermal Analyzer under nitrogen atmosphere with a flow rate of 20 ml min^{-1} for 10 mg sample. Samples were heated in the temperature range of 45–850 °C with a heating rate of 10 °C min^{-1}. The specific surface area was analyzed by using the multi-point BET technique with a surface area analyzer instrument (Thermo Finnigan Qsurf Series). Pyridine FTIR spectra were recorded using a Perkin Elmer Spectrum One FT-IR spectrometer. Solid sample (10–15 mg) was pressed into a self-supporting wafer of 13 mm diameter and preactivated under vacuum (10^{-6} mbar) at 200 °C for 3 h. The background spectrum was recorded first after cooling the sample to room temperature. The pyridine was then introduced to the sample for 5 min, then consequently desorbed at 150, 250 and 350 °C. Finally, the spectrum was recorded with a 4 cm^{-1} resolution and 10 scans in the range of 1700–1400 cm^{-1}.

2.4. Catalytic experiments

The reactions were conducted under atmospheric pressure in a 100 ml double-necked round bottom as follows: benzoyl chloride (10 ml) as the acylating agent was mixed with biphenyl (1.0 mmol) in the flask and magnetically stirred under nitrogen gas flow. The freshly activated SO_4-AlMCM-41 catalyst (0.5 g) was added and the reaction was allowed to heat at 180 °C and refluxed. Samples were periodically collected and analyzed by GC (Thermofinnigan's Chrom-Card S/W for Trace/Focus™ GC) equipped with a flame ionization detector (FID) and a non-polar capillary column (Equity 1), carrier gas nitrogen. The same procedure was performed with concentrated sulphuric acid (30 μl) and H-AlMCM-41 (0.5 g) as the catalysts.

3. Results and discussion

XRD patterns of *uncal*-AlMCM-41, *cal*-AlMCM-41, H-AlMCM-41 and SO_4-AlMCM-41 are shown in Fig. 1(a)–(d), respectively. Each exhibits an intense signal at $2\theta = 2.2°$ due to (1 0 0) plane and weak signals between 3.5° and 6.0° due to (1 1 0), (2 0 0) and (2 1 0) planes. These peaks confirm the hexagonal mesophase of the MCM-41 materials. More than three diffraction peaks are resolved in each of the XRD diffractograms of *uncal*-AlMCM-41, *cal*-AlMCM-41 and

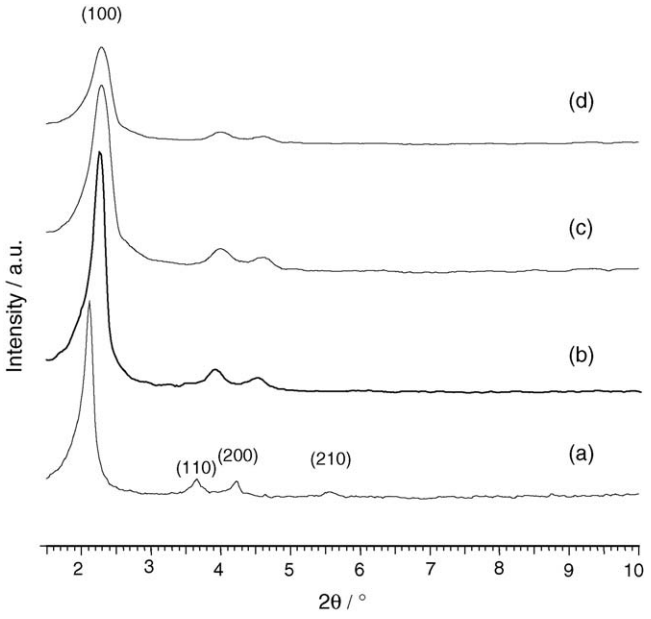

Fig. 1. X-ray diffractogram patterns of (a) *uncal*-AlMCM-41; (b) *cal*-AlMCM-41; (c) H-AlMCM-41; and (d) SO_4-AlMCM-41.

Table 1
Surface properties of MCM-41 molecular sieves

Samples	*d*-spacing (Å)	a_o (Å)	Surface area ($m^2\ g^{-1}$)	Pore volume ($cm^3\ g^{-1}$)	Acidity[a] ($\mu mol\ g^{-1}$)	
					Brønsted	Lewis
Uncal-AlMCM-41	44.07	50.88	–	–	–	–
Cal-AlMCM-41	39.81	45.97	–	–	–	–
H-AlMCM-41	38.16	44.06	1079	0.79	19.8	43.5
SO_4-AlMCM-41	37.89	43.75	549	0.28	112.9	–

[a] Acidity of samples was measured at 250 °C.

H-AlMCM-41, implying highly ordered structures. As a consequence of template removal upon calcination, the intensity of the (1 0 0) peak increases and shifts to a lower *d*-value, indicating more ordered framework structure and a decrease in the unit cell parameters, respectively.

It is also observed that the structural order of MCM-41 material changes after treatment with NH_4NO_3 and H_2SO_4. After ion-exchange with NH_4NO_3, there is a decrease in intensity of the (1 0 0) peak of H-AlMCM-41, indicating a decrease in the order of the mesoporous structure. Comparatively, the intensity of peaks in the XRD pattern for SO_4-AlMCM-41 (Fig. 1(d)) is further reduced and broadened, suggesting either a partial loss of structural order or possible decrease in the particle size of the sulphated MCM-41 material. As indicated by the surface properties data shown in Table 1, there is not much change in the unit cell parameters of the sample upon sulphation. However, there is a marked decrease in pore volume and surface area of the SO_4-AlMCM-41 sample relative to the H-AlMCM-41 sample. This strongly suggests that sulphate groups have been successfully immobilized in the pore of MCM-41.

The infrared spectra of the *uncal*-AlMCM-41, *cal*-AlMCM-41, H-AlMCM-41 and SO_4-AlMCM-41 molecular sieves are presented in Fig. 2(a)–(d), respectively. The broad peak around 3420 cm^{-1} is due to O–H stretching of water; the bands at around 2924 and 2854 cm^{-1} shown in Fig. 2(a) are assigned to symmetric and asymmetric stretching modes of the C–H sp^3 groups of the organic template. The corresponding bending mode of C–H is observed at 1480 cm^{-1}. The peak at around 1640 cm^{-1} corresponds to bending mode of O–H. The peaks around 1229 and 1084 cm^{-1} are attributed to the asymmetric stretching of Si–O–Si groups. The symmetric stretching modes of Si–O–Si groups are observed at around 799 and 578 cm^{-1}. The peak at 965 cm^{-1} is assigned to the presence of defective Si–OH groups, while the adsorption band at 455 cm^{-1} corresponds to the bending vibration of Si–O–Si or Al–O–Si groups. Fig. 2(b) also shows that the symmetric and asymmetric modes of the C–H sp^3 group of the template are absent in the spectra of calcined samples, indicating that the organic template has been removed successfully. The IR spectrum of SO_4-AlMCM-41 material in Fig. 2(d) shows a few additional peaks. The additional band at 1288 cm^{-1} corresponds to the stretching vibration of the S=O bond, and the absorption band at 1179 cm^{-1} is due to symmetric vibrations of Si–O–S bridges. In addition, the band observed at 884 cm^{-1} is assigned to symmetric S–O stretching vibrations, whereas the band at 806 cm^{-1} is assigned to symmetric Si–O stretching mode. The SO_2 deformation frequency has been assigned in the region 580 cm^{-1} [12,17]. Thus, all these results indicate that the sulphuric acid has been successfully anchored on the walls of AlMCM-41.

The TG profile of the *uncal*-AlMCM-41, H-AlMCM-41 and SO_4-AlMCM-41 materials are depicted in Fig. 3. Basically, the TG of *uncal*-AlMCM-41 sample follows a three-stage weight

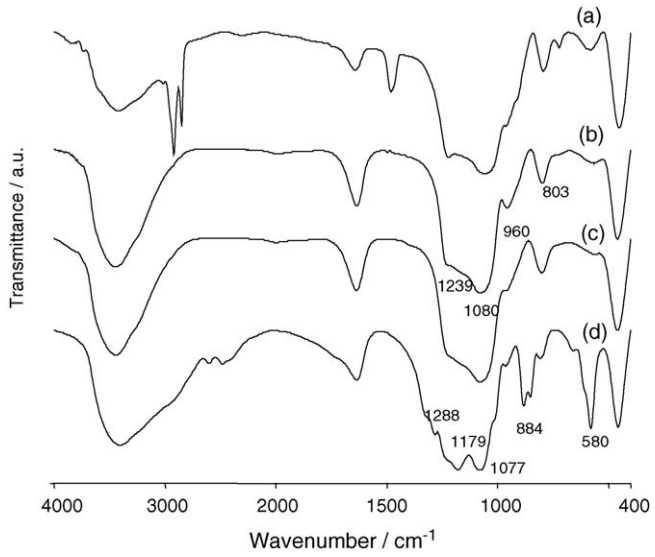

Fig. 2. Infrared spectrum of (a) *uncal*-AlMCM-41; (b) *cal*-AlMCM-41; (c) H-AlMCM-41; and (d) SO_4-AlMCM-41.

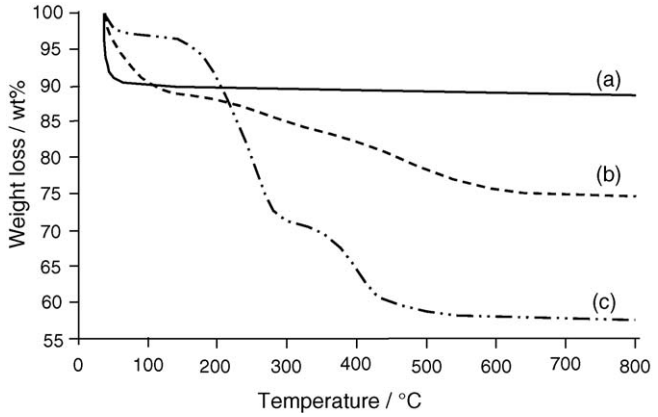

Fig. 3. Thermogravimetric analysis of (a) H-AlMCM-41; (b) SO_4-AlMCM-41; and (c) *uncal*-AlMCM-41 samples in nitrogen gas with 20 °C/min heating rate.

loss. The first stage loss (around 5%) was due to desorption of water and adsorption of gas molecules (<200 °C). In the second stage, a high-temperature weight loss peak (−33%) at 200–450 °C was also observed, which corresponds to the decomposition of template in the samples via Hofmann elimination. The third stage weight loss (∼3%) was due to water produced by thermal condensation of silanol groups to siloxane groups (450–550 °C) [18]. Meanwhile, SO_4-AlMCM-41 shows two additional and distinct weight losses, at 200–300 and 300–600 °C, due to the decomposition of sulphate groups attached to MCM-41 molecular sieves. The four-steps weight loss observed for SO_4-AlMCM-41 further verifies the interaction between the sulphate groups with the surface of MCM-41.

Fig. 4(a) shows the ^{27}Al MAS NMR spectrum of SO_4-AlMCM-41. The spectrum reveals the presence of peaks only at 0 ppm, assigned to octahedrally coordinated aluminium. It is interesting to note that the peak at 54 ppm which corresponds to tetrahedral aluminium of the framework is not observed [9,10]. The disappearance of the peak corresponding to tetrahedral aluminium indicates that after treatment with sulphuric acid, tetrahedrally coordinated aluminium was removed from the framework and transformed to octahedral aluminium, generally referred as extraframework aluminium (EFAL). However, detail examination of SO_4-AlMCM-41 spectrum reveals the presence of two peaks: a strong peak at 0 ppm and a weak peak at −5 ppm, suggesting the existence of octahedrally coordinated aluminium with two different chemical environments. These peaks might originate from EFAL present in the form of either Al^{3+}, AlO^+, $Al_x(OH)_y^{n+}$ or $Al_x(OSO_3H)_y^{n+}$. The ^{27}Al MAS NMR spectrum for SO_4-AlMCM-41 after treatment with 1.0 M methanolic HCl solution, as shown in Fig. 4(d) does not exhibit any peak at the range of 0 ppm, confirming that the origin of both aluminium are extraframework.

In order to assign the two peaks observed in the sulphated AlMCM-41, quantitative ^{27}Al MAS NMR whereby a sample containing a mixture of both sulphated AlMCM-41 and aluminium sulphate (50:50) was used. Knowing that aluminium in aluminium sulphate is octahedral, we therefore matched one of the peaks to octahedral aluminium found in aluminium sulphate [19]. The spectrum in Fig. 4(a) shows that there exist two types of Al in the sulphated AlMCM-41 sample: the peak at 0 ppm is due to nonframework octahedral aluminium in aluminium sulphate, while the peak at −5 ppm is due to octahedral aluminium bonded to EFAL (SiO–Al $(OSO_3H)_5^{n+}$). SiO^- attached to SiO–Al $(OSO_3H)_5^{n+}$ is less electronegative than SO_4^{2-} attached to aluminium sulphate and causes more shielding on the Al. Consequently, the signal which corresponds to EFAL would be shifted to a more negative chemical shift value. This further supports the data by TG analysis, where two distinct weight losses observed, at 200–300 and 300–600 °C, were presumably due to the decomposition of SiO–Al $(OSO_3H)_5^{n+}$ and aluminium sulphate, respectively.

Conventionally, Lewis acidity is attributed to octahedrally coordinated aluminum. Since the peak for tetrahedral aluminium was not observed by ^{27}Al MAS NMR, therefore Brönsted acidity was not expected to exist in SO_4-AlMCM-41. However, this implication contradicts that made by the pyridine-FTIR spectroscopy. Fig. 5(a) and (b) shows the pyridine-FTIR spectra of SO_4-AlMCM-41 and H-AlMCM-41, respectively. It is observed that H-AlMCM-41 exhibits bands at 1546 cm^{-1} assigned to pyridine bound to Brønsted acid sites and at 1455 cm^{-1} assigned to pyridine bound to Lewis acid sites [10]. This agrees with the results by ^{27}Al MAS NMR (Fig. 4(b)) where tetrahedral framework Al attributed to Brønsted acid sites and octahedral extraframework Al attributed to Lewis acid sites were observed.

^{27}Al MAS NMR studies of SO_4-AlMCM-41 sample in Fig. 4(a) did not show the presence of tetrahedral framework Al. In contrast, Fig 5(a) of SO_4-AlMCM-41 sample, showed no Lewis acid sites but possess high amount of Brønsted acid sites instead. Therefore, the existence of Brønsted acid sites in this sample, which has never been observed in similar system before, must be due to the introduction of sulphate group ($HOSO_3-$) into the sample that may have formed bond with the octahedral aluminium. The peak intensity ratio of aluminium

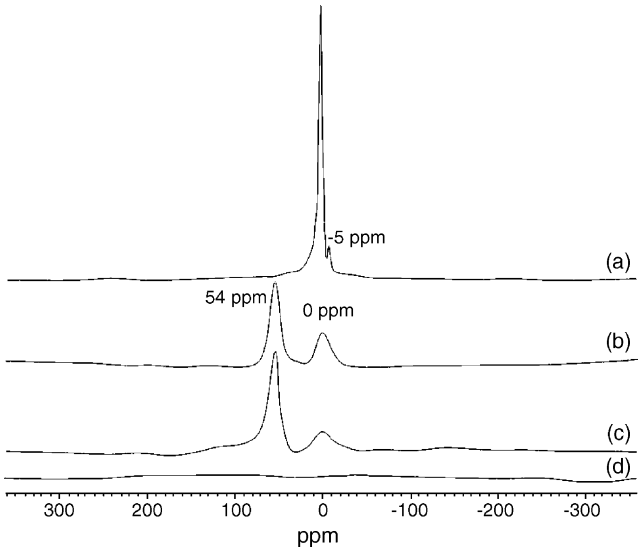

Fig. 4. ^{27}Al MAS NMR spectra of (a) SO_4-AlMCM-41; (b) H-AlMCM-41; (c) *cal*-AlMCM-41; and (d) SO_4-AlMCM-41 after treatment with 1.0 M methanolic HCl solution.

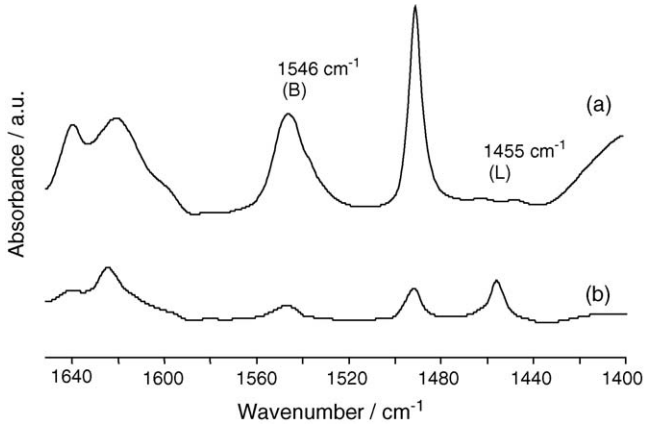

Fig. 5. The pyridine-FTIR spectra of (a) SO_4-AlMCM-41 and (b) H-AlMCM-41 at 250 °C.

Table 2
Benzoylation and dibenzoylation of biphenyl (BP) with benzoyl chloride over various types of catalysts at 180 °C for 24 h

Catalyst(s)	Conversion of BP (%)	Selectivity towards 4-PBP (%)	Selectivity towards 4,4′-DBBP (%)	Selectivity towards others (%)
H_2SO_4[a]	75.0	35.3	0.0	39.7
H-AlMCM-41	83.7	83.7	0.0	0.0
H_2SO_4 + H-AlMCM-41	90.6	13.0	1.65	76.0
SO_4-AlMCM-41	94.2	83.2	11.0	0.0
SO_4-silica	22.3	22.1	0.0	0.2

[a] Homogeneous catalyst, (4-PBP), 4-benzoylbiphenyl and (4,4′-DBBP), 4,4′-dibenzoylbiphenyl.

sulphate to EFAL, calculated from the ^{27}Al MAS NMR spectrum of SO_4-AlMCM-41, is 9:1. Since there was a large increase in the amount of Brönsted acid sites formed upon sulphation (Fig. 5(a)), therefore, it can be concluded that both nonframework aluminium sulphate and EFAL provide the sites for the formation of Brønsted acid. Besides, the intensity of the IR signal at 3740 cm^{-1} attributed to silanol group decreased significantly after treatment with sulphuric acid (Fig. 6). This further indicates that the sulphate groups not only reacted with Al–OH but also with Si–OH groups, which consequently enhanced the amount of Brønsted acid sites.

The results of our studies show that the types of acid sites formed are influenced by the use of different solvents during sulphation of AlMCM-41. In all studies reported earlier, sulphation was performed in aqueous environment [12–16]. In contrast, our system was conducted in hydrophobic environment. Water which is a hydrophilic solvent would hydrolyze the sulphate groups attached to the AlMCM-41, producing Lewis acid sites. However, hydrophobic organic solvent such as dehydrated toluene which was used in this work, successfully protected the sulphate groups from being hydrolyzed and hence produced Brønsted acid sites.

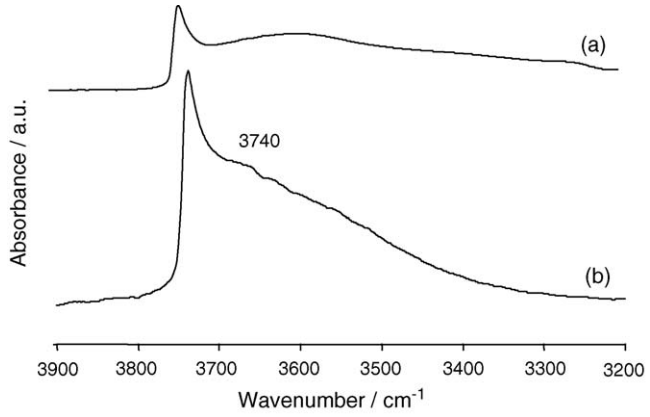

Fig. 6. FTIR spectra of silanol groups of MCM-41 materials at 250 °C: (a) H-AlMCM-41 and (b) SO_4-AlMCM-41.

The activity of SO_4-AlMCM-41 catalyst was tested in the Friedel-Crafts dibenzoylation reaction. In the absence of catalyst, the rate of benzoylation was very slow and dibenzoylation totally did not occur. Catalytic test results shown in Table 2 indicate that in the presence of H-AlMCM-41 catalyst, the biphenyl conversion was 83.7%. Unfortunately, the H-AlMCM-41 catalyst was inactive towards dibenzoylation of biphenyl and was unable to produce disubstituted product within 24 h. The results suggest that either the acidity of the catalyst was not strong enough or the amount of acid sites was not large enough to convert biphenyl to 4,4′-DBBP. Concentrated sulphuric acid shows 75.0% conversion of biphenyl but with poorer selectivity (35.3%) towards benzoylation. Benzoylation of biphenyl using two catalysts, H-AlMCM-41 and concentrated sulphuric acid simultaneously, gave 90.6% conversion of biphenyl but low selectivity (13.0% of 4-PBP and 1.65% of 4,4′-DBBP). On the other hand, sulphuric acid incorporated in fully amorphous silica with surface area of 43.06 cm^2 g^{-1} was only able to give 22.3% conversion of biphenyl and produced 22.1% of 4-PBP.

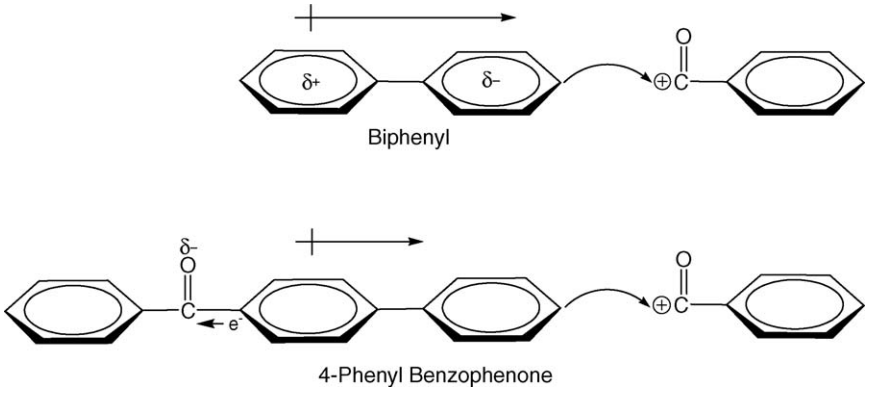

Fig. 7. The effect of electron density on the attack of the benzoylium ion on biphenyl (BP) and 4-phenyl benzophenone (4-PBP).

Evidently, SO_4-AlMCM-41 exhibited remarkable activity and selectivity. The catalyst was able to convert 94.2% of biphenyl into 83.2% of 4-PBP within 24 h, proving high performance towards benzoylation and 11.0% selectivity towards 4,4′-DBBP with no side products. The highest selectivity achieved by SO_4-AlMCM-41 was attributed to the uniform mesopores of 3 nm in diameter present in the MCM-41 molecular sieves, which enabled it to reduce the accumulation of the bulkier *ortho*- and *meta*-substituted products. Such phenomenon is called shape-selective effect.

The results in Table 2 also show that 4,4′-DBBP was produced when the conversion of BP exceeded 90%. This phenomenon is not only related to the amount of BP and 4-PBP in the system but also the electron density factor. The electron density in 4-PBP is lower than BP due to dislocation of electrons, which deactivates the attack of benzoylium ion by 4-PBP in order to form disubstituted 4,4′-DBBP. On the other hand, BP with higher electron density tends to attack benzoylium ion to form 4-PBP. The attack on benzoylium ion by 4-PBP becomes dominant when the concentration of BP is very low. Fig. 7 demonstrates how BP and 4-PBP attack benzoylium ion.

4. Conclusions

Sulphated AlMCM-41 (SO_4-AlMCM-41) mesoporous molecular sieves with SiO_2/Al_2O_3 ratio = 15 was prepared via impregnation of sulphuric acid using an organic solvent on the surface of H-AlMCM-41. Results of this work demonstrate that SO_4-AlMCM-41 is a solid Brønsted acid and active towards benzoylation and dibenzoylation of biphenyl. The production of 4,4′-DBBP is affected by the amount of acid site, amount of biphenyl and 4-PBP. The SO_4-AlMCM-41 was found to be active towards dibenzoylation of biphenyl reaction, giving 11.0% of 4,4′-DBBP, whereas sulphuric acid and H-AlMCM-41 catalyst only produced 4.1% of 4,4′-DBBP.

Acknowledgements

The authors would like to acknowledge the Ministry of Science, Technology and Innovation of Malaysia for financial support.

References

[1] G.D. Yadav, M.S. Krishnan, Chem. Eng. Sci. 54 (1999) 4189.
[2] A.P. Singh, D. Bhattacharya, S. Sharma, J. Mol. Catal. A 102 (1995) 139.
[3] B. Jacob, S. Suguman, A.P. Singh, J. Mol. Catal. A 139 (1999) 43.
[4] T. Raja, A.P. Singh, A.V. Ramaswamy, A. Finiels, P. Moreau, Appl. Catal. A: Gen. 211 (2001) 31.
[5] D. Bhattacharya, S. Sharma, A.P. Singh, Appl. Catal. A: Gen. 150 (1997) 53.
[6] M. Chidambaran, C. Venkatesan, P. Moreau, A. Finiels, A.V. Ramaswamy, A.P. Singh, Appl. Catal. A: Gen. 224 (2002) 129.
[7] W.J. Feast, I.S. Millichamp, Polym. Commun. 24 (1983) 102.
[8] J.H. Burroughes, D.D.C. Bradley, A.R. Brown, R.N. Marks, K. Mackay, R.H. Friend, P.L. Burns, A.B. Holmes, Nature 347 (1990) 539.
[9] R.R. Mukti, M.Sc. thesis, Universiti Teknologi Malaysia, Johor, Malaysia, 2003.
[10] R.R. Mukti, N. Hadi, S. Endud, H. Hamdan, Stud. Surf. Sci. Catal. (2004) 2767.
[11] M. Chidambaram, D. Curulla-Ferre, A.P. Singh, B.G. Anderson, J. Catal. 220 (2003) 442.
[12] M. Selvaraj, M.P.K. Sinha, A. Pandurangan, Micropor. Mesopor. Mater. 70 (2004) 81.
[13] M. Selvaraj, K. Lee, K.S. Yoo, T.G. Lee, Micropor. Mesopor. Mater. 81 (2005) 343.
[14] M. Selvaraj, P.K. Sinha, K.S. Seshadri, A. Pandurangan, Appl. Catal. A: Gen. 265 (2004) 75.
[15] M. Selvaraj, A. Pandurangan, K.S. Seshadri, P.K. Sinha, V. Krishnasamy, K.B. Lal, J. Mol. Catal. A 192 (2003) 153.
[16] Li-Wen Chen, Chih-Yu Chou, An-Nan Ko, Appl. Catal. A: Gen. 178 (1999) L1–L6.
[17] C.N.R. Rao, Chemical Applications of Infrared Spectroscopy, Academic Press, New York, 1963, p. 296.
[18] M. Busio, J. Jänchen, H.H.C. van Hooff, Micropor. Mater. 5 (1995) 211.
[19] J.T. Kloprogge, P.J.J. Dirken, B.H. Jansen, J.W. Geus, J. Non-Cryst. Solids 181 (1995) 151.